# Base Sequence Dependence of in Vitro Translesional DNA Replication past a Bulky Lesion Catalyzed by the Exo$^-$ Klenow Fragment of Pol I†

Ping Zhuang,‡ Alexander Kolbanovskiy,‡ Shantu Amin,§ and Nicholas E. Geacintov*,‡

*Chemistry Department, New York University, 31 Washington Place, New York, New York 10003-5180, and American Health Foundation, Valhalla, New York 10595*

*Received January 2, 2001; Revised Manuscript Received March 14, 2001*

ABSTRACT: The effects of base sequence, specifically different pyrimidines flanking a bulky DNA adduct, on translesional synthesis in vitro catalyzed by the Klenow fragment of *Escherichia coli* Pol I (exo$^-$) was investigated. The bulky lesion was derived from the binding of a benzo[*a*]pyrene diol epoxide isomer [(+)-*anti*-BPDE] to $N^2$-guanine (G*). Four different 43-base long oligonucleotide templates were constructed with G* at a site 19 bases from the 5′-end. All bases were identical, except for the pyrimidines, X or Y, flanking G* (sequence context 5′-...XG*Y..., with X, Y = C and/or T). In all cases, the adduct G* slows primer extension beyond G* more than it slows the insertion of a dNTP opposite G* (A and G were predominantly inserted opposite G*, with A > G). Depending on X or Y, full lesion bypass differed by factors of ∼1.5−5 (∼0.6−3.0% bypass efficiencies). A downstream T flanking G* on the 5′-side instead of C favors full lesion bypass, while an upstream C flanking G* is more favorable than a T. Various deletion products resulting from misaligned template−primer intermediates are particularly dominant (∼5.0−6.0% efficiencies) with an upstream flanking C, while a 3′-flanking T lowers the levels of deletion products (∼0.5−2.5% efficiencies). The kinetics of (1) single dNTP insertion opposite G* and (2) extension of the primer beyond G* by a single dNTP, or in the presence of all four dNTPs, with different 3′-terminal primer bases (Z) opposite G* were investigated. Unusually efficient primer extension efficiencies beyond the adduct (approaching ∼90%) was found with Z = T in the case of sequences with 3′-flanking upstream C rather than T. These effects are traced to misaligned slipped frameshift intermediates arising from the pairing of pairs of downstream template base sequences (up to 4−6 bases from G*) with the 3′-terminal primer base and its 5′-flanking base. The latter depend on the base Y and on the base preferentially inserted opposite the adduct. Thus, downstream template sequences as well as the bases flanking G* influence DNA translesion synthesis.

Benzo[*a*]pyrene (B[*a*]P),[1] a widespread environmental pollutant, is metabolized in vivo to a variety of mutagenic derivatives (*1*) that form bulky DNA adducts. The most genotoxic metabolite of B[*a*]P is the diol epoxide (+)-7*R*,8*S*-dihydroxy-9*S*,10*R*-epoxy-7,8,9,10-tetrahydrobenzo[*a*]pyrene [(+)-*anti*-BPDE]. This stereoisomer is known to form covalent adducts with native DNA mainly by *trans*-addition of the exocyclic amino group of guanine to the C10 position of BPDE (*2*) to form the covalent (+)-*trans*-*anti*-[BP]−$N^2$-dG adduct depicted in Figure 1. While these DNA lesions strongly block DNA replication (*3*, *4*), mutagenic bypass is well established in prokaryotic and eukaryotic cells treated with BPDE (*5*−*8*). The effects of base sequence on error-prone DNA replication past bulky DNA lesions, especially [BP]−$N^2$-dG adducts, has been studied extensively but is still not well understood (*9*, *10*).

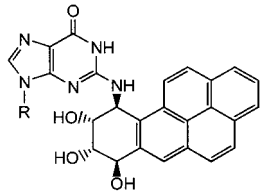


(+)-*trans*-*anti*-[BP]-$N^2$-dG

FIGURE 1: Structure and absolute configuration of the *anti*-[BP]−$N^2$-dG adduct (G*).

The availability of site-specifically modified oligonucleotides with single, stereochemically defined [BP]−$N^2$-dG lesions positioned in different base sequence contexts (*11*−*13*) has stimulated a number of site-specific mutagenesis studies in vitro (*14*−*18*) and in cellular systems (*19*−*24*). The mutagenic properties of the [BP]−$N^2$-dG adducts depend on the adduct stereochemistry, the base sequence context, and the cell system in which the mutations are expressed (*16*, *19*−*23*, *25*, *28*). The most frequently observed base substitution mutations are G → T transversions in prokaryotic

† This research was supported by the U.S. Public Health Service, National Cancer Institute, National Institutes of Health, Grant CA-76660 awarded by the Department of Health and Human Services. The diol epoxide (±)-*anti*-BPDE was obtained from the National Cancer Institute Carcinogen Reference Standard Repository.

* Corresponding author: Tel. (212) 998-8407; fax (212) 998-8421; e-mail ng1@nyu.edu.

‡ New York University.

§ American Health Foundation.

[1] Abbreviations: BP, benzo[*a*]pyrene; (+)-*anti*-BPDE, (+)-7*R*,8*S*-dihydroxy-9*S*,10*R*-epoxy-7,8,9,10-tetrahydrobenzo[*a*]pyrene; (+)-*trans*-*anti*-[BP]−$N^2$-dG, adduct derived from the binding of (+)-*anti*-BPDE to the exocyclic amino group of a 2′-deoxyguanosine residue in DNA; EDTA, ethylenediaminetetraacetate; dNTP, 2′-deoxynucleoside 5′-triphosphate.

10.1021/bi010005o CCC: $20.00 
Published on Web 05/02/2001

Chart 1[a]

**a. Running-start primer extension:**

```
                    Four dNTPs
                         ←          CGATAGACCGGTC-5'        (13mer)
5'-GACTACGTACTGT CACAXG*YACACGCTATCTGGCCAGATCCGC  (43mer)
          10        19          30        40
```

**b. Insertion opposite the lesion site:**

```
                  Single dNTP
                         ↓ WTGTGCGATAGACCGGTC-5'        (18mer)
5'-GACTACGTACTGT CACAXG*YACACGCTATCTGGCCAGATCCGC  (43mer)
```

**c. Extension past the lesion site:**

```
                    dNTP
                         ↓ Z WTGTGCGATAGACCGGTC-5'      (19mer)
5'-GACTACGTACTGT CACAXG*YACACGCTATCTGGCCAGATCCGC  (43mer)
```

[a] X, Y = C or T; Z = A, G, C, or T; W is complementary to Y.

(16, 19−22, 24, 25) and in eukaryotic cells (20, 21). However, G → A and G → C mutations, have also been observed in some base sequence contexts (18−22, 26). The mutagenic specificities observed with site-specific (+)-*trans-anti*-[BP]−N2-dG lesions generally reflect the kinds of mutations observed in random mutagenesis experiments, i.e., when cells are treated with (+)-*anti*-BPDE (6, 8, 27). On the basis of the results of site-directed mutagenesis experiments, Loechler and co-workers (7, 28) have advanced the hypothesis that different adduct conformations can give rise to different kinds of base substitution mutations and that these conformations strongly depend on base sequence context.

Since many experiments can be performed in a relatively short period of time, site-directed mutagenesis experiments in vitro, employing purified polymerases, represent a useful approach for studying base sequence effects on bypass of the (+)-*trans-anti*-[BP]−$N^2$-dG lesion (G*). The effects of different bases flanking the adduct G* on translesional bypass have not yet been analyzed systematically. However, such studies have been performed with *N*-(deoxyguanosin-8-yl)−2-acetylaminofluorene and −2-aminofluorene lesions (*29*, *30*). In this work we focus on a series of four 43-mer oligonucleotides, each with identical bases except for two pyrimidines, X and Y, flanking the lesions G*. These four sequences, designated as XG*Y = TG*C, CG*C, TG*T, and CG*T (Chart 1), were used as templates in primer extension reactions in vitro catalyzed by *Escherichia coli* Pol I [Klenow fragment, $exo^-$ ($KF^-$)]. The exonuclease-deficient Klenow fragment was selected because the proofreading mechanism itself may introduce base sequence-dependent effects (*31*). Although $KF^-$ is primarily involved in DNA repair, it is a simple, well-characterized peptide with high replication fidelity (*32*). A thorough characterization of base sequence effects on lesion bypass catalyzed by $KF^-$ should provide an interesting basis for making similar comparisons with other prokaryotic or eukaryotic polymerases, including the recently discovered bypass polymerases (*33*−*35*) that bypass (+)-*trans-anti*-[BP]−$N^2$-dG lesions in vitro (*35*, *36*) and in vivo (*24*). In our 43-mer template strands, the lesions G* are positioned 19 nucleotides from the 5′-end, thus allowing for a rather long single-stranded overhang in the template−primer complexes bound to the polymerase. This design was adopted because short overhangs, with G* only five bases from the 5′-end of the template strand, diminish the binding of $KF^-$ to DNA (*37*). The (+)-*trans-anti*-[BP]−$N^2$-dG lesions strongly block primer extension beyond the modified guanine, as found earlier in vitro with different, shorter template−primer sequences (*14*−*18*). The efficiencies of translesion bypass, giving rise to fully extended primer strands can vary by as much as a factor of ∼6 as the nature of the pyrimidines flanking the lesion is changed. However, the efficiencies of translesional bypass resulting in frameshifted primer extension products (deletion products) depend not only on the bases flanking the lesion but also on the more distant 5′ downstream base sequence context on the template strand.

Chart 2[a]

```
        13mer        11mer          19mer
          |            |              |                |
5'-GACTACGTACTGT CACAXG*YACAC GCTATCTGGCCAGATCCGC  (43-mer)
    GATGCATGACA GTGTW'CWTGTG CGATAGACCGGTCTAGG-5'  (39-mer)
```

X, Y=C, T.

[a] X, Y = C or T.

## MATERIALS AND METHODS

*Chemicals and Enzymes.* All chemicals were analytical grade. [$\gamma$-$^{32}$P]ATP (3000 ci/mmol) was purchased from NEN Life Science Products, Inc. DNA polymerase I Klenow fragment ($exo^-$), T4 polyneocleotide kinase, and T4 ligase were obtained from Amersham Life Science, Inc. The dNTPs were purchased from New England Biolabs, Inc. The concentration of the Klenow fragment was 10 units/$\mu$L, where one unit catalyzes the incorporation of 10 nmol of dNTP $s^{-1}$ into a poly(dA)•poly(dT) substrate.

*BPDE-Modified DNA Oligodeoxynucleotides*. All oligonucleotides were synthesized on a Biosearch Cyclone DNA synthesizer and were purified by standard HPLC protocols (*38*). Site-specifically modified 11-mer oligonucleotides (Chart 2) with single (+)-*trans-anti*-[BP]−$N^2$-dG lesions were generated by a direct synthesis method (*11*) using racemic *anti*-BPDE obtained from the National Cancer Institute Carcinogen Reference Standard Repository. The procedures used and the methods of characterization and verification of adduct stereochemistry were the same as those previously described for one of the 11-mer sequences (*39*) used in this work. The 11-mers were ligated to a 13-mer and a 19-mer to form the 43-mer template strand. The three oligonucleotides were hybridized with a complementary 39-mer (Chart 2). The BPDE-modified 11-mer (3 nmol) and the 19-mer were phosphorylated at the 5′-end with 1.5 mM ATP, in a 1× T4 polynucleotide kinase buffer, and 20 units of T4 polynucleotide kinase in a volume of 20 $\mu$L. The mixture was incubated at 37 °C for 40 min. The reaction was stopped by heating at 90 °C for 5 min and then desalted by ethanol precipitation. The phosphorylated 19-mer and BPDE-modified 11-mer were then incubated with equal amounts of the 13-mer and a 39-mer complementary strand in a 200 $\mu$L solution containing 50 mM Tris-HCl, 10 mM $MgCl_2$, 10 mM DTT, and 1.5 mM ATP. The mixture was brought to 90 °C for 5 min and was then slowly cooled to room temperature and finally to 4 °C, and 15 units of T4 DNA ligase was added. The ligation was carried out at 4 °C for 16 h and then stopped by addition of 30 $\mu$L of 100 mM EDTA. The sample was reheated at 90 °C for 5 min, followed by rapid chilling on ice, and then purified on a 20% polyacrylamide gel with 7 M urea. The 43-mer template bands were visualized by ethidium bromide staining and

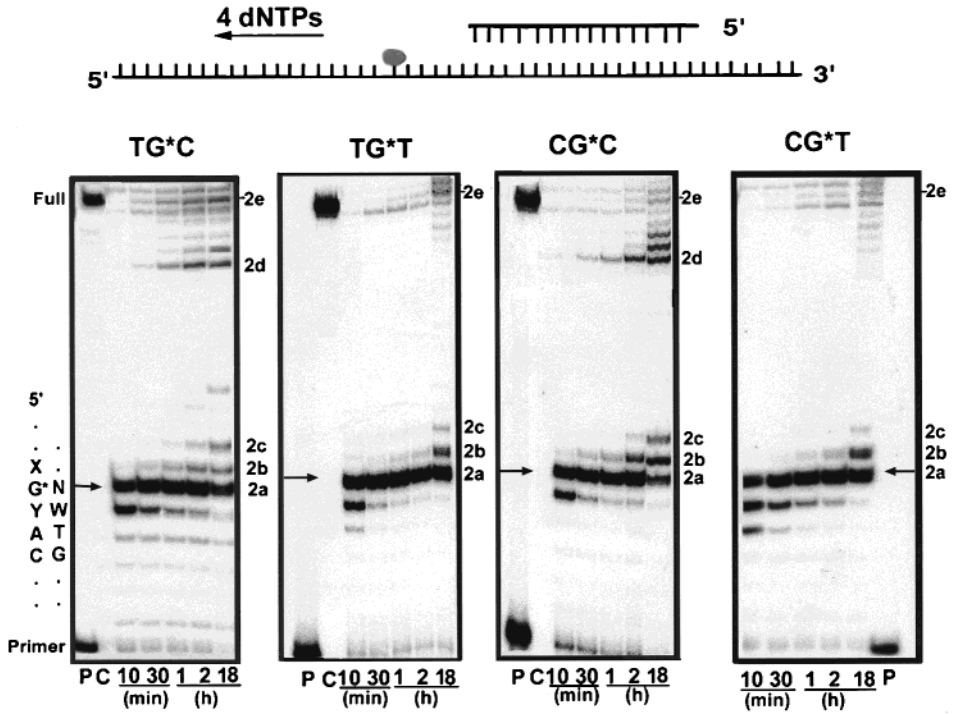


FIGURE 2: Running-start time course primer extension reactions. $^{32}$P-Labeled 13-mer primers were extended (Chart 1a) in the presence of all four dNTPs (see text for conditions). Lanes labeled P represent the 13-mer primers; lanes labeled C represent the 37-mer, full extension products. Bands 2a−2e were excised and eluted from the gels and subjected to Maxam−Gilbert sequencing analysis, and each type of band (a, b, etc.) had the same composition. The position of the 19-mer primer extension product (successful incorporation of a dNTP, N, opposite G* into the primer) is indicated by an arrow.

excised, and the DNA was eluted and precipitated with ethanol.

*Running-Start DNA Replication.* The 43-mer templates were annealed with a $^{32}$P-labeled 13-mer primer as shown in Chart 1a. The BPDE-modified guanine residue was positioned at template position 25 counted from the 3′ end of the template strand. The time course of primer extension assays of the adducted templates with the Klenow fragment of DNA polymerase I (exo$^-$), KF$^-$, was carried out at 25 °C in 30 $\mu$L of buffered solution containing 60 nM primer−template complexes, 120 $\mu$M dNTPs, and 1 $\mu$L of 10 units/$\mu$L KF$^-$ in 1× polymerase reaction buffer. The reactions were stopped after preselected time intervals by addition of an equal amount of stop solution (20 mM EDTA in 95% formamide) to the reaction mixture. The mixtures were then heated at 90 °C for 5 min, chilled on ice, and then applied to a 20% denaturing polyacryalmide gel containing 7 M urea. The bands were visualized by autoradiography employing a Bio-Rad GS-525 phosphoimager.

*Single dNTP Insertion opposite the Template Lesion Site.* The 43-mer template containing BPDE-modified dG was annealed with a $^{32}$P-labeled 18-mer primer. The site-specific insertion reactions with single dNTP (dATP, dGTP, dCTP, or dTTP) and KF$^-$ were carried out at 25 °C in 30 $\mu$L of a buffered solution containing 60 nM primer−template complexes, 250 $\mu$M single dNTP, and 1 $\mu$L of 10 units/$\mu$L KF$^-$ for 20 min (Chart 1b).

*Primer Extension past the Lesion Site.* The 43-mer templates were annealed with a $^{32}$P-end-labeled 19-mer containing either an A, G, C, or T at the 3′-terminus (Chart 1c). The elongation reactions with all four dNTPs and KF$^-$ were carried out at 25 °C in a 30 $\mu$L buffer solution containing 60 nM primer−template complexes, 120 $\mu$M dNTPs, and 1 $\mu$L of 10 units/$\mu$L KF$^-$ in 1× polymerase reaction buffer for 1 h and 18 h, respectively.

*Kinetics Studies.* The Michaelis−Menten parameters $V_{max}$ and $K_m$, characterizing single-base insertion opposite the modified guanine, G*, and one-base extension past G* (Chart 1b,c), were measured under conditions similar to those described earlier (*15*). The 43-mer templates were annealed with a $^{32}$P-labled primer (an 18-mer for insertion kinetics and a 19-mer for extension kinetics) in a solution of 50 mM Tris-HCl (pH 8.0), 5 mM $MgCl_2$, and 2 mM $\beta$-mercaptoethanol. The polymerase (0.05−5 nM KF, exo$^-$) and dNTPs (in the range of 0.01−1 $\mu$M with unmodified templates and 2−200 $\mu$M in the case of BPDE-modified templates) were added to initiate the reactions. The reactions were stopped after time intervals varying from 60 s to 40 min, and under conditions when no more than 20% primer extension had occurred. The kinetic parameters were obtained from standard Hanes−Woolf plots (*40*).

## RESULTS

*Running-Start DNA Replication (Chart 1a).* Typical results from running-start replication experiments with all four dNTPs present are shown in Figure 2. When the extension was conducted on unmodified template−primer complexes under identical conditions, each of the primers was extended completely to full-length 37-mer products within 10 min (data not shown). In the case of the BPDE-modified templates, primer extension from the 13-mer to an 18-mer (the 3′-terminal primer base extended up to the base flanking the lesion on the upstream side), is quite rapid, while the 18-mer → 19-mer primer extension is significantly slower. The 18-mer band disappears in all cases after a reaction time of ∼2 h (Figure 2). Primer extension beyond the 19-mer

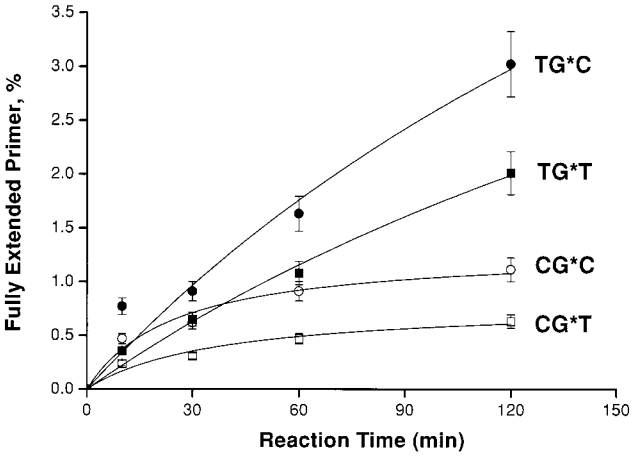


FIGURE 3: Formation of full primer extension products (37- and 38-mers) as a function of reaction time (from autoradiographs of data in Figure 2, average of two separate runs).

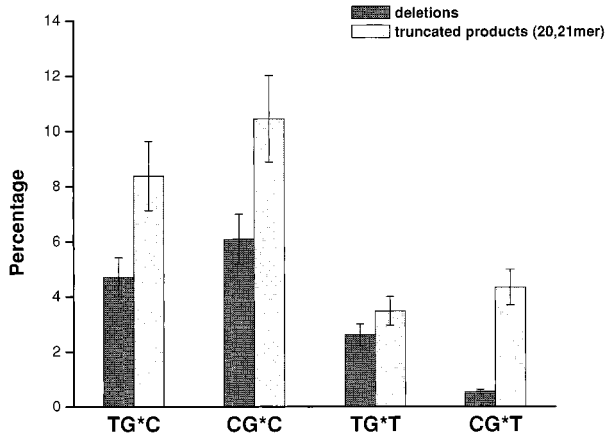


FIGURE 4: Percentages of primers forming deletions and truncated extension products after a reaction time of 2 h (data from Figure 2).

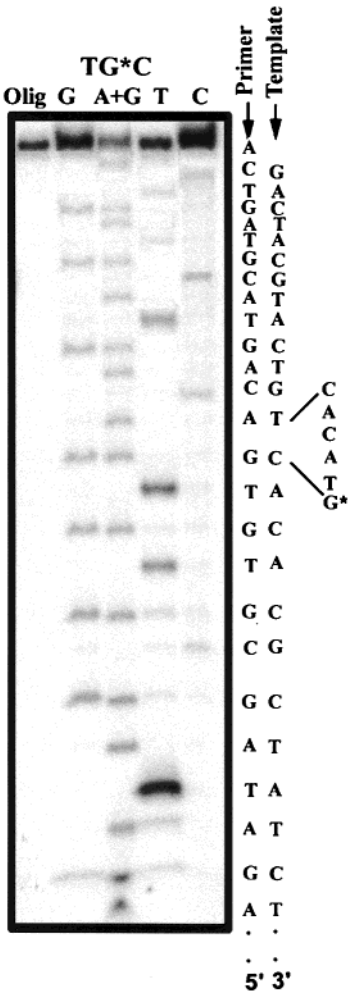


FIGURE 5: Maxam−Gilbert sequencing of six-base primer extension deletion product (designated as band 2d in Figure 2) obtained with the TG*C template strand. The primer sequence and the template strand segment not replicated are shown on the right.

results in several kinds of extension products. The time course of formation of full extension products is shown in Figure 3. Small amounts, ∼0.6−3.0% of fully extended 37-mers and 38-mers, are observed after a 2 h reaction time. The 38-mers result from the blunt-end addition of an A to the 3′-end of the primer (*41*). The amounts of fully extended products follow the order TG*C > TG*T > CG*C > CG*T (Figure 3). Shorter primer extension products include various extended primer deletion products 32−36 bases long. The formation of these deletion products is more efficient in the case of the TG*C and CG*C sequences (∼5% and 6%, respectively) than in the case of the TG*T (2.5%) and CG*T (0.5%) sequences (Figure 4). The most abundant bypass products are the truncated 20- and 21-mer primer extension products (Figure 4). The highest fractions (∼8% and 10%) are observed in the case of the TG*C and CG*C sequences, when the lesion is flanked by a C on the upstream side. After a 2-h reaction time, the overall lesion bypass was ∼16−17% in the case of the TG*C and CG*C sequences and ∼8% and ∼5% in the case of TG*T and CG*T sequences, respectively.

*Maxam−Gilbert Sequencing of Running-Start Primer Extension Products.* The primer extension products labeled 2a−2e in Figure 2 were subjected to Maxam−Gilbert sequencing (*42*). The 19-mer extended primer product 2a (Figure 2) derived from the TG*C template, has a G and an A (A > G) at the 3′-terminus, showing that dATP and dGTP are inserted opposite the lesion site (Figure S1, Supporting Information). Similar results were obtained for the 19-mers 2a in the case of the other three sequences (data not shown).

Maxam−Gilbert sequencing of the 20- and 21-mer primer extension products (primer bands 2b and 2c in Figure 2) show that these contain mostly A and some G at sites 20 and 21 (Figure S2, Supporting Information). The polymerase adds one or two additional As (or some Gs) beyond the lesion site and further extension ceases, yielding the observed truncated 20- and 21-mer extension products.

Sequencing of the band 2d shows that this is a 32-mer primer extension deletion product (Figure 5). The base sequence of this product is consistent with a model in which the template strand six-base sequence 5′-...ACATG*C... was not copied by the polymerase.

In all fully extended primers (37- and 38-mers, bands 2e in Figure 2), the only abnormal bases detected by Maxam−Gilbert methods were A and, to a lesser extent, G inserted opposite the BPDE-modified guanine residue (data not shown). No dCTP or dTTP insertion opposite the adduct was observed by the Maxam−Gilbert methods in any of the extended primers sequenced. These sequencing results indicate that the fully extended primer strands do not arise from extension of unmodified sequences that might have

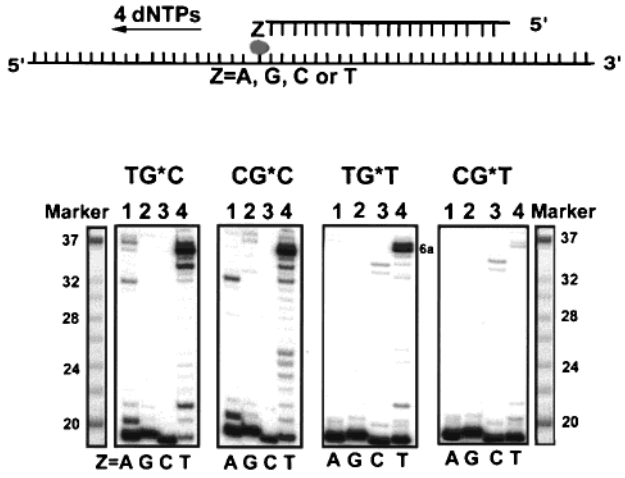


FIGURE 6: Primer extension beyond the lesion site with all four dNTPs and with different bases (Z) at the primer 3′-termini (Chart 1c). The ladders on the left and right are commercial standard-size markers (8−32 bases, from Amersham Life Science, Inc.). The 37-mer is a full primer extension product obtained in primer extension reactions with the unmodified 43-mer sequences as templates. The band designated as 6a was subjected to Maxam−Gilbert sequencing analysis.

been present as impurities in the BPDE-modified 43-mer template samples (*43*).

*Single dNTP Incorporation opposite BPDE-Modified dG.* The gel electrophoresis autoradiograms for the insertion of each of the four dNTPs, one at a time, opposite the modified guanines in each of the four different sequence contexts are shown in Figure S3, Supporting Information. While there is some sequence dependence, the general order of dNTP insertion opposite G* follows the order dATP > dGTP> dTTP > dCTP, as observed in other sequence contexts (*15, 18*).

*Primer Extension past the BPDE-Modified Lesion dG*.* Primer extension past the BPDE-modified guanine residue G* was investigated by use of all four dNTPs and 19-mer primers with different bases, Z, at the 3′ termini positioned opposite G*. Figure 6 shows typical gel autographs representing primer extension products after reaction times of 1 h. With Z = T at the 3′-terminus of the primer strand opposite G* (G*•T), and particularly in the sequences TG*C, CG*C, and TG*T, primer extension is significantly more efficient than in the case of Z = A, G, or C. The primer extension products 6a (see labeled bands in Figure 6) were sequenced and were shown to be predominantly 36-mers, or −2 deletion primer extension products (data not shown). Primer extension in the case of the CG*T sequence is weakest with either of the four bases at the 3′-end of the primer strand opposite G*. Small amounts of full-length extension products (37- or 38-mers) are observed in the TG*C (G*•A) and CG*C (G*•G) cases. No significant amounts of full-length extension products were observed in the TG*T or CG*T sequences, regardless of the nature of Z. Shorter deletion products were observed in most experiments (Figure 6) but were not studied in detail.

*Determination of Single dNTP Insertion Efficiencies ($f_{ins}$) opposite G* (Chart 1b).* The values of the parameters $V_{max}$, $K_m$, and $f_{ins} = V_{max}/K_m$ were evaluated in order to ascertain whether sequence effects influence primarily $V_{max}$ or $K_m$, or both. Some typical values of these parameters are summarized in Table 1. More extensive results are provided in Figures S4 and S5 (Supporting Information). The relative efficiencies of insertion of dNTPs opposite G*, $f_{ins}$, are compared for the four different sequences in Figure 7a. The $f_{ins}$ values for dNTP insertion are $\sim 10^3-10^4$ times smaller in the case of templates with G* than with the unmodified G. This difference can be attributed primarily to the much larger values of $K_m$ observed in the case of the modified template strands G* than to the influence of the BP residues on $V_{max}$ (see examples in Table 1).

For insertion of dATP opposite the lesion, the values of $f_{ins}$ are ∼1.5−2.0 times greater for the two sequences with a T rather than a C at the downstream 5′-side of the lesion. The $f_{ins}$ value for the insertion of dATP opposite the lesion are uniformly (3−5 times) larger than for the insertion of dGTP, and only minor effects of flanking base sequences can be discerned. The $f_{ins}$ value for insertion of dTTP is ∼10 times smaller than in the case of dATP in the TG*C, TG*T, and CG*T sequences but is ∼50 times smaller in the CG*C sequence context. The lowest efficiencies of insertion, particularly in the CG*C and TG*C sequences, are observed in the case of insertion of dCTP opposite G* ($f_{ext}$ ∼30−80 times smaller than for dATP insertion).

*Extension by One dNTP past the Lesion Site G* (Chart 1c).* Some typical values of $V_{max}$ and $K_m$, for modified and unmodified templates (G* and G at position 19, respectively), with Z = A at the 3′-end of the primer strand are presented in Table 1. Other values of these parameters are shown in Figure S5, Supporting Information. All $f_{ext}$ values are summarized in Figure 7b. In all cases, the $V_{max}$ and $K_m$ values for primer extension past the lesion site were determined for the insertion of the next correct base after the lesion G*, i.e., dGTP in the case of CG*C and CG*T and dATP in the case of TG*T and TG*C (Figure S5, Supporting Information). The $f_{ext}$ values for the extension of the primer strands past the lesion site with different bases, Z, at the 3′-end of the primer and opposite G* exhibit greater variability as a function of template sequence context then the insertion of dATP or dGTP opposite the lesion (Figure 7).

In the case of the template−primer G*•A mismatch at the primer terminus, the $f_{ext}$ values for primer extension past the lesion are at least 1 order of magnitude smaller than for the insertion of dATP opposite the lesion and at least 4 orders of magnitude smaller than in the case of primer extension beyond a normally base-paired and unmodified G•C terminus (Table 1). The $f_{ext}$ values (Figure 7) are lower for extension past G*•A with an upstream 3′-flanking T (TG*T and CG*T) than a 3′-flanking C (CG*C and TG*C).

With Z = G, the $f_{ext}$ value was too small to be measured in the case of the CG*T sequence. A rather strong effect of base sequence is observed in the other oligonucleotides with the $f_{ext}$ values arranged in the order TG*T > TG*C > CG*C > CG*T (Figure 7b). For a single-base extension past a G*•G terminus in the CG*C, TG*C, and TG*T sequences, the values of $V_{max}$ values are ∼10 times smaller than the $V_{max}$ values for the insertion of dGTP opposite G*. However, the $K_m$ values are particularly unfavorable in the case of the CG*C and TG*C sequences (Figure S5). These sequence-dependent variations in $K_m$ account predominantly for the strong sequence dependence of $f_{ext}$.

Table 1: Some Examples of Kinetic Parameters Determined for Primer Insertion or Primer Extension beyond the Modified Guanine Residue (G*) by a Single dNTP (Chart 1b,c)[a]

| insertion of dNTP | sequence | $V_{max}$ | $K_m$ | $f_{ins}$ |
|---|---|---|---|---|
| dCTP | CGC (um) | 12 ± 1.0 | 0.030 ± 0.003 | 390 ± 75 |
| dATP | CG*C | 3.4 ± 0.5 | 15 ± 2.2 | 0.23 ± 0.05 |
| dATP | TG*C | 6.0 ± 0.9 | 15 ± 2.1 | 0.41 ± 0.08 |

| extension by dNTP | | base X opposite G (G•X or G*•X) | $V_{max}$ | $K_m$ | $f_{ext}$ |
|---|---|---|---|---|---|
| dGTP | CGC (um) | G•C | 3.1 ± 0.7 | 0.033 ± 0.005 | 95 ± 32 |
| dGTP | CGC (um) | G•A | 2.3 ± 0.8 | 0.036 ± 0.008 | 64 ± 21 |
| dGTP | CG*C | G*•A | 0.12 ± 0.02 | 11.6 ± 1.7 | 0.011 ± 0.002 |
| dGTP | CG*C | G*•T | 4.0 ± 0.6 | 0.062 ± 0.009 | 64 ± 13 |
| dATP | TG*C | G*•A | 0.32 ± 0.05 | 27 ± 4.1 | 0.012 ± 0.002 |
| dATP | TG*C | G*•T | 2.4 ± 0.4 | 0.037 ± 0.006 | 66 ± 13 |
| dATP | TG*T | G*•T | 0.036 ± 0.005 | 4.4 ± 0.7 | 0.0082 ± 0.002 |
| dGTP | CG*T | G*•T | 0.71 ± 0.1 | 13 ± 2.0 | 0.055 ± 0.01 |

[a] Um, unmodified sequences. $V_{max}$ is given in units of percent primer extended per minute; $K_m$ is given in micromolar units.

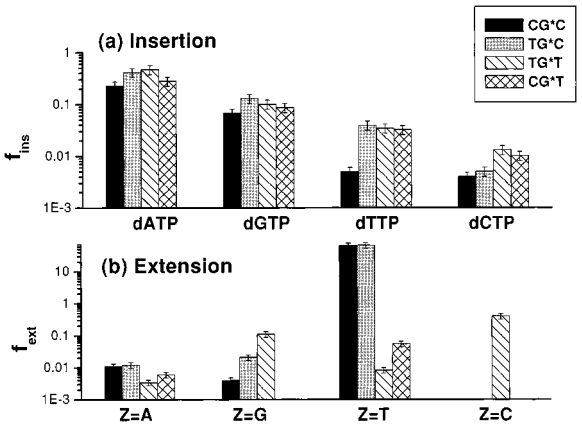


FIGURE 7: Base sequence dependence of the steady-state single dNTP insertion opposite G* ($f_{ins}$) and single dNTP extension (either dATP or dGTP, depending on template base flanking G* on the downstream (5′) side ($f_{ext}$), with $f = V_{max}/K_m$ (some values of $V_{max}$ and $K_m$ are shown in Table 1, with the rest shown in Figures S4 and S5, Supporting Information).

In the case of Z = C, an $f_{ext}$ value was measurable only in the case of the TG*T sequence. The $f_{ext}$ values were <0.001 for the other three sequences.

The most striking impact on primer extension past the lesion is observed in the case of Z = T (G*•T template−primer terminus). This effect is particularly important in the case of the CG*C and TG*C sequences since, in both cases, the $V_{max}$ values are very high [(4.0 ± 0.6) and (2.4 ± 0.4) % $min^{-1}$, respectively] and the $K_m$ values are very small (0.062 ± 0.01 and 0.037 ± 0.006 $\mu$M, respectively). These values combine into the highest values of $f_{ext}$ [∼(65 ± 13) % $min^{-1}$ $\mu M^{-1}$), close to the values observed with unmodified DNA (Table 1). While in the case of the CG*T sequence the value of $V_{max}$ is relatively high [(0.71 ± 0.1) % $min^{-1}$], the value of $K_m$ is also high, thus leading to a relatively unfavorable $f_{ext}$ value for single base extension past a G*• T terminus. In the TG*T sequence, $V_{max}$ is low [(0.036 ± 0.005) % $min^{-1}$] and $K_m$ is high (4.4 ± 0.7 $\mu$M), thus giving rise to the smallest value of $f_{ext}$ for primer extension past a G*•T terminus (Figure 7).

## DISCUSSION

*Polymerase Stall Sites and Adduct Conformations*. The polymerase first stalls when the 3′-terminal base in the primer strand is paired with the pyrimidine base Y that flanks G* on the upstream side (Figure 2). Dzantiev and Romano (*44*, *45*) recently suggested that bulky aromatic lesions at the polymerase active site inhibit the rate-determining conformational change in the polymerase that is required for the incorporation of a nucleotide. It has been shown by NMR techniques that in similar primer−template complexes, the hydrophobic BP residue is stacked with the 3′-terminal G on the primer strand, while the modified guanine is in a *syn* rather than in the usual *anti* conformation (*46*). Assuming that this stacking interaction persists at the active site of the polymerase complex, the slow insertion of dNTPs opposite G is reasonable since the modified guanine moiety occupies approximately the position normally assumed by the incoming dNTP. A recent molecular modeling study reveals that even if the BP-modified guanine residue at the active site of the polymerase is in the *anti* conformation, the orientation of the BP-modified guanine residue is still unfavorable for dNTP insertion (*47*). Insertion of dCTP, or another dNTP, would require a conformational change of the (+)-*trans*-*anti*-[BP]−$N^2$-dG adduct, which could be a rare though not completely improbable event (*10*). The insertion of the dNTP could then allow the conformational change of the polymerase to occur *(44, 45)*.

The extent of lesion bypass is different in the four sequences studied (Figures 3 and 4). In all cases, the slowest step is the extension of the primer beyond the site of the lesion. A similar pattern of stall sites was found with $KF^-$ in the case of the less bulky 1,$N^2$-ethenoguanine and 1,$N^2$-ethanoguanine adducts (*48*). An NMR study of the solution conformation of a (+)-*trans*-*anti*-[BP]−$N^2$-dG adduct at a single strand/double strand junction with the 3′-terminal primer base opposite G* in a ...CG*C... sequence context shows that this C forms a Watson−Crick base pair with the guanine residue of G* (*49*). The BP residue is no longer stacked with one of the DNA bases and, instead, points into the downstream, 5′-side of the modified template strand, thus hindering the approach of the dNTP to the next template base to be replicated. With Z = C opposite G*, significant primer extension by a single dNTP beyond the lesion occurs only in the case of the TG*T sequence (Figure 7b). This unusual sequence effect is associated with a relatively favorable value of $V_{max}$ rather than a low value of $K_m$ and may be related to the unusual flexibility of the TG*T

sequences (*50*). This flexibility may allow for a conformational mobility at the primer−template junction, which may favor an adduct conformation that is associated with more efficient primer extension beyond the lesion (*10*).

*Effects of Bases Flanking the Adduct on Lesion Bypass.* The probability of lesion bypass resulting in the formation of fully extended primers (Figure 3) is more efficient in the TG*C and TG*T sequences, i.e., with a T flanking the adduct on the downstream side.

Since A is preferentially inserted opposite G* in all sequences, the more favorable effect of a downstream T flanking the lesion on full bypass (Figure 2) may be related to a slipped misaligned intermediate proposed for translesion primer extension catalyzed by Pol $\beta$ (*51, 52*). Slippage of the modified guanine may allow for the formation of a "dATP-stabilized misalignment" intermediate (*51*):

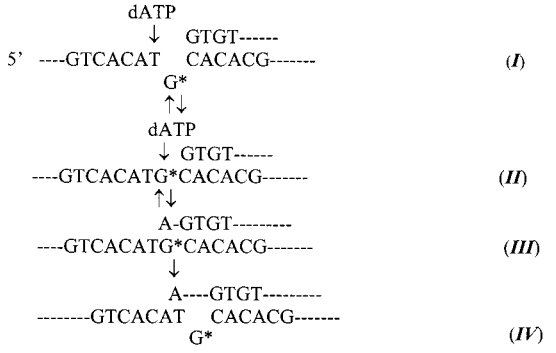


The misaligned intermediate *I* might facilitate incorporation of A opposite G* (II) to form *III*. This mechanism may account for the somewhat higher values of $f_{ins}$ for the insertion of dATP opposite G* in the TG*C and TG*T than in the CG*C and CG*T sequences (Figure 7a). Further extension from *III* can occur with the incorporation of another dATP. If the slipped frameshift intermediate *IV* is formed, the insertion of dTTP opposite the first downstream template A residue would result in a (−1) deletion product upon further primer extension.

*Effect of Upstream Pyrimidine Bases Flanking G**. With a T on the upstream side of G* and either a C or a T on the 5′-side, full bypass is lower than with a C flanking the modified guanine on the 3′-side (Figure 3). While this effect is not large in the case of our (+)-*trans*-*anti*-BPDE−$N^2$-dG lesion, much larger adverse effects of upstream flanking Ts have been observed by Efrati et al. (*51*) for translesional bypass of abasic sites; the frequency factors $f_{ins}$ for inserting A opposite the abasic sites catalyzed by pol α and pol $\beta$ were some 10−20 times greater with an upstream C rather than an upstream T flanking the lesion site on the 3′-side (*51*). Unfavorable effects of an upstream T flanking a propano-dG lesion (*53*) and an $O^6$-methylguanine lesion (*54*) on lesion bypass have also been reported. It is shown in the Supporting Information that substitution of single C·G base pairs by T·A base pairs flanking G* thermodynamically destabilizes the DNA duplexes. Therefore, one might expect more fraying of the base pair with T·A rather than C·G base pairs at the template−primer junction. However, it is unclear whether this effect is related to the decreased lesion bypass in the TG*T and CG*T versus the TG*C and CG*C sequences (Figures 3 and 4).

*dNTP Insertion opposite G**. Maxam−Gilbert sequencing of this partially extended 19-mer primer product indicates that the base inserted opposite the lesion is predominantly A or G with A > G (Figure S1, Supporting Information). These results are consistent with the favorable dATP insertion kinetics opposite G* (Figure 7a), corresponding to the well-known "A"-rule (*55*), and with earlier in vitro results in other sequences (*15, 16, 18*).

In general, low values of $f_{ins}$ opposite G*, when compared to unmodified sequences, are due to relatively large values of $K_m$ rather than to decreased values of $V_{max}$ (Table 1), thus suggesting a $K_m$ discrimination mechanism (*56, 57*). In the absence of proofreading, high values of $K_m$ might suggest a higher rate constant of dissociation of the dNTP from the active site of the polymerase (*58*), although it is well-known that the significance of $K_m$ values is generally ambiguous because of the complexity of the kinetics (*59*). The insertion of dATP opposite G* shows the least variation as a function of base sequence. While $V_{max}$ is larger with an upstream 3′-C rather than a T flanking the adduct, the associated $K_m$ are also larger (Figure S4, Supporting Information). As a result, the $f_{ins}$ exhibits only small variations as a function of base sequence (Figure 7a).

*Base Sequence Dependence of Formation of Deletion Products.* We show here that the downstream sequence context at some distance from the lesion G* is critical to the formation of misaligned slipped intermediates and the formation of deletion primer extension products. The deletions and truncated products are formed more efficiently with Y = C than with Y = T flanking the lesion on the upstream side. Various deletion mechanisms involving stalled template−primer/polymerase complexes have been studied previously (*29, 57, 60, 61*). Similar principles can also account for the occurrence of deletion products upon extension of the appropriate misaligned template−primer intermediates in the TG*C and CG*C sequences. Here we consider some examples of slipped frameshift intermediates that can account for the observed deletion primer extension products.

The shortest deletion primer extension products are 32-mers (bands 2d in Figure 2). These are observed when the lesion site G* is flanked by an upstream C rather than by an upstream T (TG*C and CG*C). As shown in Figure 5, these 32-mers arise from a (−6) deletion intermediate (the base sequence of bands 2d are identical to one another in the case of TG*C and CG*C). In the TG*C sequence, for example, the appearance of the (−6) deletion product can be accounted for in terms of the following examples of misaligned frameshift intermediates with Z = A:

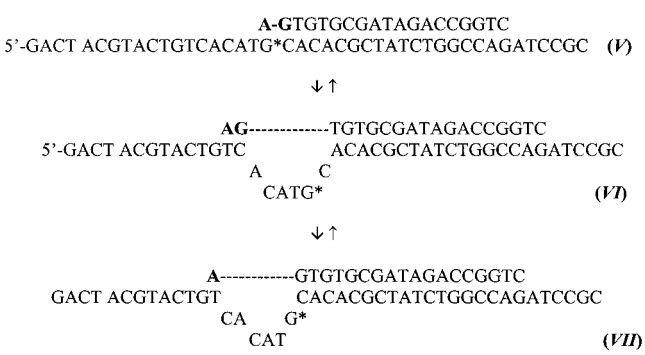

Successful extension from *V* would produce full-length primer extension, while extension from *VI* (or *VII*) would lead to the observed (−6) deletion products. Insertion of a G opposite G* would not favor a slippage mechanism in the case of the TG*C and CG*C sequences, since there are no downstream CC template sequences for the 3′-GG... primer bases to pair with. Similarly, insertion of A opposite G* in the case of TG*T and CG*T would yield two AA bases at the 3′-end of the primer; however, there are no downstream TT template bases to pair with, so (−6) deletion products are not observed in these sequences either.

It can be shown that longer primer extension products with (−1), (−2), (−3), (−4), and (−5) deletion primer products are also possible by extension of misaligned intermediates in the case of primers with Z = A, G, or T at their 3′-termini (Chart 1c). However, the identities of these primer extension products were not the primary focus of this work, and this topic was therefore not pursued in detail.

*Truncated Primer Extension Products*. In all four sequences, the 19-mer is slowly and partially extended to a 20- or 21-mer, most likely by the insertion of A opposite G* (Figure 7a). In the case of the sequences with a T flanking the lesion on the 5′-side, these 20/21-mer truncated primers may arise from slipped frameshift intermediates in which a primer A residue, rather than G*, is looped out of the primer−template duplex and may be in equilibrium with other misaligned intermediates.

```
          A
          A  GTGT…..-5’
5’…….CACATG*CACA…..        (VIIIa)
          ↑↓
          AA GTGT…..-5’
5’…….CACAT  CACA…..        (VIIIb)
          G*
          ↑↓
          AA-GTGT…..-5’
5’…….CACATG*CACA…..        (VIIIc)
```

With a C flanking the lesion on the 5′-side, an A is inserted opposite G*, followed by the insertion of a G that pairs with the C on the template strand, as reported earlier by Shibutani et al. (*15*) for a similar sequence. The truncated extension products arise because further primer extension is inhibited when there are two or more mispaired bases at the 3′-end of the primer.

*Base Sequence Dependence of Primer Extension Efficiency beyond the Site of the Lesion*. The efficiencies of primer extension beyond the site of the lesion depend remarkably not only on Z, the base at the 3′-terminus of the primer strand opposite G* (Chart 1c), but also on the pyrimidines flanking the lesion and the downstream base sequence context (Figure 6). When all four dNTPs are present, full-length primer extension products 37 or 38 bases long are observed after a 1 h reaction time (Figure 6) only with Z = A (TG*C), and with Z = G, T, or A (CG*C); no full-length products are observed when a T flanks the lesion on the upstream side (TG*T and CG*T). Particularly striking is the efficient primer extension observed in the case of Z = T, i.e., from a G*•T template−primer terminus in the case of the TG*C, CG*C, and TG*T sequences (Figure 6). In the case of the CG*C and TG*C sequences, this is consistent with the unusually high frequency factors, $f_{ext}$, for extension by a single dNTP (dATP) beyond the G*•T template−primer termini (Figure 7b). The $f_{ext}$ values, as well as the $V_{max}$ and $K_m$ values, for these two sequences are close in value to those observed for unmodified sequences (Table 1). This is consistent with dNTP insertion opposite a template base distant from the lesion site (sequences *VI* and *VII*). As Miller and Grollman (*62*) have shown, the site-specific primer extension frequencies 5 bases or more downstream from the lesions are expected to approach values that are characteristic of unmodified sequences. Taken together, these results indicate that the observed efficient primer extension with Z = T occurs by a misalignment mechanism. Taking the CG*C sequence as an example, the following slipped frameshift intermediate could lead to the observed deletion band (6a) in Figure 6:

```
                TG----TGTGCGATAGACCGGTC
GACTACGTACTGTCACAC    ACACGCTATCTGGCCAGATCCGC
                  G*C                        (IX)
```

This slipped frameshift intermediate would yield (−2) deletions or 35-mer (or 36-mer with blunt-end addition) primer extension products. Base pairing of the 3′-TG primer end with the next two downstream template AC base sequences would yield a (−4) deletion. A third deletion product about 32 bases long was not identified.

In the case of the TG*C sequence, the following examples of slipped frameshift intermediates can lead to a (−4) deletion:

```
                TG - - - - TGTGCGATAGACCGGTC
GACTACGTACTGTCAC       ACACGCTATCTGGCCAGATCCGC
                  ATG*C                      (X)
```

A (−2) deletion could be introduced by another frameshift intermediate, stabilized by a G•C base pair flanking the lesion site:

```
                T- - - -GTGTGCGATAGACCGGTC
GACTACGTACTGTCACA      CACACGCTATCTGGCCAGATCCGC
                  TG*                        (XI)
```

Furthermore, the 3′-TGT... bases at the end of the primer could pair with the 5′-...ACA... downstream template sequence, thus representing another pathway for forming a slipped frameshift intermediate. The intermediates *X* and *XI* can account for the two deletion products observed in the case of TG*C with Z = T. Similar deletion products should be possible in the case of the CG*T sequence but are not observed, thus suggesting that the bases flanking the lesion influence the stabilities of slipped frameshift intermediates.

With Z = T in the TG*T sequence, Maxam−Gilbert sequencing reactions of band 6a (Figure 6) is consistent with the formation of the following misaligned intermediate:

```
                TA-----TGTGTGCGATAGACCGGTC
GACTACGTACTGTCACAT    ACACGCTATCTGGCCAGATCCGC
                  G* T                       (XII)
```

In the CG*T sequence context with Z = T, the two 3′-terminal primer strand bases are TA, but there are no template 5′-AT base sequences on the downstream side to pair with. Thus, short deletion products are not observed in this case (Figure 6).

Recently, Alekseyev and Romano (*18*) observed single-dNTP primer extension reactions beyond (+)-*trans-anti*-BPDE−$N^2$-dG lesions with oligonucleotides with a CG*T and a TG*C sequence context but with different base sequences from the ones used here. They measured the $f_{ext}$

values for extension by a single dNTP in the two template sequences 5′-d(CCATXG*YTACCGTTCCGTCGTTTTCG-TG), with X = C and Y = T in one oligonucleotide and X = T and Y = C in the other. With Z = T at the 3′-primer terminus opposite G*, they observed a very high $f_{ext}$ value in the case of their CG*T sequence (dGTP insertion opposite the flanking downstream template C) but not in the case of their TG*C sequence (insertion of dATP opposite T). This is exactly the opposite of our results, since TG*C with Z = T is more easily extended than CG*T (Figure 6). However, this seeming contradiction can be explained by examining the downstream template sequences of Alekseyev and Romano. On the 5′-side of G*, one of their sequences is 5′-CCATCG*T...-3′, while the other is 5′-CCATTG*C...-3′; in the case of their CG*T sequence with Z = T, the two terminal primer bases, 3′-TA..., can pair with a pair of downstream 5′-...AT... template strand bases, thus forming a misaligned intermediate. However, in the TG*C sequence, the primer 3′-end bases 3′-TG... do not have any downstream 5′-...AC... base sequences to pair with, and misaligned intermediates should not be favored. Thus, the differences in the one-dNTP primer extension efficiencies in their sequences and in ours can be entirely attributed to differences in the base sequence context on the downstream side of the template strand.

Overall, these results suggest that such measurements of $f_{ext}$ values for single base extension beyond the lesion site with different bases Z opposite the adduct G* should not be used to predict the efficiencies of full primer extension and the preferred (Z) base substitution mutation. Such measurements *(18)* must be complemented by extension experiments with all four dNTPs in order to gain a true picture of the relative contributions of base substitutions to full primer extension and deletion mutations. The effects of downstream template sequences on primer extension efficiencies when slipped frameshift intermediates can arise has been also discussed earlier by Goodman and co-workers (*63*), who studied the impact of abasic sites on polymerase kinetics.

*Mutational Characteristics of* (+)-*trans-anti-[BP]*−$N^2$-*dG Lesions in Vivo*. When the *supF* gene of an *E. coli* plasmid is treated with (+)-*anti*-BPDE, G → T mutations are dominant in SOS-induced *E. coli* cells (*7*). Site-directed mutagenesis studies in *E. coli* show that G → T mutations also dominate in a 5′-TG*C-3′ sequence context (*25*), a CG*G context (*19*), CG*A and GG*T sequence contexts (*22*), a TG*G context (*20*), a GG*A context (*24*), CG*G and GG*C sequence contexts (*16*), and a GG*C sequence context in mammalian COS cells (*20*). In all four of our sequences, G → T mutations are also predicted to be dominant (Figure 7a), as observed in vitro in other experiments (*15, 16*). However, G → A mutations dominate in a CG*T (*26, 64*) and a 5′-AG*A-3′ sequence context (*65*) in *E. coli*. Since we tested both the TG*C and CG*T sequences and found that insertion of dATP opposite G* is dominant in both cases, other factors besides the flanking bases must obviously govern the mutagenic specificity of (+)-*trans-anti*-[BP]−$N^2$-dG lesions. These differences could include host factors (*43*), e.g., the SOS-induced *umuDC* (pol V) and *dinB* (pol IV) translesion bypass polymerases in *E. coli* (*24*). In addition, Moriya et al. (*20*) have shown that cellular prokaryotic and eukaryotic polymerases process the (+)-*trans-anti*-[BP]−$N^2$-dG lesions quite differently.

Here we have shown that the more distant bases strongly influence lesion bypass by a slipped frameshift intermediate mechanism. Deletion mutations in vivo arising from translesion bypass of (+)-*trans-anti*-[BP]−$N^2$-dG lesions (*24*) or DNA treated with (+)-*anti*-BPDE (*7, 8, 27*) have been reported. Generally, frameshift mutations and large deletions occur in runs of purines, especially guanines (*66*). However, translesion bypass can occur by a slipped frameshift intermediate mechanism even when the modified guanines are flanked by pyrimidines on both sides (*29*). Thus, the sequence-dependent deletions observed here are not surprising, although the large 6-base deletions are unusual.

## CONCLUSIONS

The pyrimidine bases, C or T, flanking the (+)-*trans-anti*-BPDE−$N^2$-dG lesions on the 3′- or 5′-sides can exert up to a 6-fold difference on full lesion bypass. Full primer extension is favored by a downstream flanking T. On the other hand, an upstream flanking T with either a flanking C or a T on the downstream 5′-side of the adduct diminishes full primer extension. Deletion extension products (up to six deleted bases) are most prominent with an upstream 3′-flanking C. However, this type of lesion bypass is related not only to the 3′-flanking base but also to the overall template 5′-flanking base sequence context up to six bases downstream from the adduct. Highly efficient lesion bypass can depend on the formation of slipped, misaligned intermediates and have no effect on base substitution mutations since only deletion products are formed.

## ACKNOWLEDGMENT

We gratefully acknowledge the assistance of Dr. T. Liu in setting up these experiments, and we thank Dr. E. L. Loechler for fruitful discussions.

## SUPPORTING INFORMATION AVAILABLE

One table showing the melting points of 11-mer duplexes with the same central sequence context as the XG*Y sequences studied (Chart 1) and five figures showing the Maxam−Gilbert analysis of three different primer extension products and the base sequence dependence of the kinetic parameters $V_{max}$ and $K_m$ for single dNTP insertion opposite G*, and extension beyond G*, by one dNTP. This material is available free of charge via the Internet at http://pubs.acs.org.

## REFERENCES

1. Conney, A. H. (1982) *Cancer Res. 42*, 4875−4917.
2. Cheng, S. C., Hilton, B. D., Roman, J. M., and Dipple, A. (1989) *Chem. Res. Toxicol. 2*, 334−340.
3. Moore, P. D., and Strauss, B. S. (1979) *Nature 278*, 664−666.
4. Brown, W. C., and Romano, L. J. (1991) *Biochemistry 30*, 1342−1350.
5. Eisenstadt, E., Warren, A. J., Porter, J., Atkins, D., and Miller, J. H. (1982) *Proc. Natl. Acad. Sci. U.S.A. 79*, 1945−1949.
6. Yang, J.-L., Maher, V. M., and McCormick, J. M. (1987) *Proc. Natl. Acad. Sci. U.S.A. 84*, 3787−3791.
7. Rodriguez, H., and Loechler, E. L. (1993) *Carcinogenesis 14*, 373−383.
8. Wei, S. J., Chang, R. L., Hennig, E., Cui, X. X., Merkler, K. A., Wong, C. Q., Yagi, H., Jerina, D. M., and Conney, A. H. (1994) *Carcinogenesis 15*, 1729−1735.

9. Bigger, C. A. H., Ponten, I., Page, J. E., and Dipple, A. (2000) *Mutat. Res. 450*, 75−93.
10. Kozack, R., Seo, K., Jelinsky, S. A., and Loechler, E. L. (2000) *Mutat. Res. 450*, 41−59.
11. Cosman, M., Ibanez, V., Geacintov, N. E., and Harvey, R. G. (1990) *Carcinogenesis 11*, 1667−1672.
12. Lakshman, M. K., Sayer, J. M., Yagi, H., and Jerina, D. M. (1992) *J. Org. Chem. 57*, 4585−4590.
13. DeCorte, B. L., Tsarouhtsis, D., Kuchimanchi, S., Cooper, M. D., Horton, P., Harris, C. M., and Harris, T. M. (1996) *Chem. Res. Toxicol. 9*, 630−637.
14. Hruszkewycz, A. M., Canella, K. A., Peltonen, K., Kotrappa, L., and Dipple, A. (1992) *Carcinogenesis 13*, 2347−2352.
15. Shibutani, S., Margulis, L. A., Geacintov, N. E., and Grollman, A. P. (1993) *Biochemistry 32*, 7531−7541.
16. Hanrahan, C. J., Bacolod, M. D., Vyas, R. R., Liu, T., Geacintov, N. E., Loechler, E. L., and Basu, A. K. (1997) *Chem. Res. Toxicol. 10*, 369−377.
17. Lipinski, L. J., Ross, H. L., Zajc, B., Sayer, J. M., Jerina, D. M., and Dipple, A. (1998) *Int. J. Oncol. 13*, 269−273.
18. Alekseyev, Y. O., and Romano, L. J. (2000) *Biochemistry 39*, 10431−10438.
19. Jelinsky, S. A., Liu, T., Geacintov, N. E., and Loechler, E. L. (1995) *Biochemistry 34*, 13545−13553.
20. Moriya, M., Spiegel, S., Fernandes, A., Amin, S., Liu, T., Geacintov, N., and Grollman, A. P. (1996) *Biochemistry 35*, 16646−16651.
21. Fernandes, A., Liu, T., Amin, S., Geacintov, N. E., Grollman, A. P., and Moriya, M. (1998) *Biochemistry 37*, 10164−10172.
22. Page, J. E., Zajc, B., Oh-hara, T., Lakshman, M. K., Sayer, J. M., Jerina, D. M., and Dipple, A. (1998) *Biochemistry 37*, 9127−9137.
23. Chary, P., Latham, G. J., Robberson, D. L., Kim, S. J., Han, S., Harris, C. M., Harris, T. M., and Lloyd, R. S. (1995) *J. Biol. Chem. 270*, 4990−5000.
24. Lenne-Samuel, N., Janel-Bintz, R., Kolbanovskiy, A., Geacintov, N. E., and Fuchs, R. P. P. (2000) *Mol. Microbiol. 38*, 299−307.
25. Mackay, W., Benasutti, M., Drouin, E., and Loechler, E. L. (1992) *Carcinogenesis 13*, 1415−1425.
26. Shukla, R., Liu, T., Geacintov, N. E., and Loechler, E. L. (1997) *Biochemistry 36*, 10256−10261.
27. Rodriguez, H., and Loechler, E. L. (1993) *Biochemistry 32*, 1759−1769.
28. Loechler, E. L. (1995) *Mol. Carcinogen. 13*, 213−219.
29. Shibutani, S., and Grollman, A. P. (1993) *J. Biol. Chem. 268*, 11703−11710.
30. Shibutani, S., Suzuki, N., Tan, X., Johnson, F., and Grollman, A. P. (2001) *Biochemistry 40*, 3717−3722.
31. Goodman, M. F., and Fygenson, D. K. (1998) *Genetics 148*, 1475−1482.
32. Johnson, K. A., and Steitz, T. A. (1994) *Annu. Rev. Biochem. 63*, 777−822.
33. Woodgate, R. (1999) *Genes Dev. 13*, 2191−2195.
34. Baynton, K., and Fuchs, R. P. P. (2000) *Trends Biochem. Sci. 25*, 74−79.
35. Zhang, Y., Yuan, F., Wu, X., Wang, M., Rechkoblit, O., Taylor, J.-S., Geacintov, N. E., and Wang, Z. (2000) *Nucleic Acids Res 28*, 4138−4146.
36. Zhang, Y., Yuan, F., Wu, X., Rechkoblit, O., Taylor, J.-S., Geacintov, N. E., and Wang, Z. (2000) *Nucleic Acids Res. 28*, 4717−4724.
37. Rechkoblit, O., Amin, S., and Geacintov, N. E. (1999) *Biochemistry 38*, 11834−11843.
38. McLaughlin, W., and Piel, N. (1984) in *Oligonucleotide Synthesis: A Practical Approach* (Gait, M. J., Ed.) IRL Press, Oxford, U.K.
39. Geacintov, N. E., Cosman, M., Mao, B., Alfano, A., Ibanez, V., and Harvey, R. G. (1991) *Carcinogenesis 12*, 2099−2108.
40. Randall, S. K., Eritja, R., Kaplan, B. E., Petruska, J., and Goodman, M. F. (1987) *J. Biol. Chem. 262*, 6864−6870.
41. Clark, J. M., Joyce, C. M., and Beardsley, G. P. (1987) *J. Mol. Biol. 198*, 123−127.
42. Maxam, A. M., and Gilbert, W. (1980) *Methods Enzymol. 65*, 499−560.
43. Loechler, E. L. (1996) *Carcinogenesis 17*, 895−902.
44. Dzantiev, L., and Romano, L. J. (2000) *Biochemistry 39*, 356−361.
45. Dzantiev, L., and Romano, L. J. (2000) *Biochemistry 39*, 5139−5145.
46. Cosman, M., Hingerty, B. E., Geacintov, N. E., Broyde, S., and Patel, D. J. (1995) *Biochemistry 34*, 15334−15350.
47. Singh, S. B., Beard, W., Hingerty, B. E., Wilson, S. H., and Broyde, S. (1998) *Biochemistry 37*, 878−884.
48. Langouet, S., Mican, A. N., Muller, M., Fink, S. P., Marnett, L. J., Muhle, S. A., and Guengerich, F. P. (1998) *Biochemistry 37*, 5184−5193.
49. Feng, B., Gorin, A., Hingerty, B. E., Geacintov, N. E., Broyde, S., and Patel, D. J. (1997) *Biochemistry 36*, 13769−13779.
50. Xu, R., Mao, B., Amin, S., and Geacintov, N. E. (1998) *Biochemistry 37*, 769−778.
51. Efrati, E., Tocco, G., Eritja, R., Wilson, S. H., and Goodman, M. F. (1997) *J. Biol. Chem. 272*, 2559−2569.
52. Efrati, E., Tocco, G., Eritja, R., Wilson, S. H., and Goodman, M. F. (1999) *J. Biol. Chem. 274*, 15920−15926.
53. Hashim, M. F., and Marnett, L. J. (1996) *J. Biol. Chem. 271*, 9160−9165.
54. Singer, B., Chavez, F., Goodman, M. F., Essigman, J. M., and Dosanjh. (1989) *Proc. Natl. Acad. Sci. U.S.A. 86*, 8271−8274.
55. Strauss, B. S. (1991) *Bioassays 13*, 79−84.
56. Goodman, M. F. (1988) *Mutat. Res. 200*, 11−20.
57. Boosalis, M. S., Mosbaugh, D. W., Hamatake, R., Sugino, A., Kunkel, T. A., and Goodman, M. F. (1989) *J. Biol. Chem. 264*, 11360−11366.
58. Petruska, J., Goodman, M. F., Boosalis, M. S., Sowers, L. C., Cheong, C., and Tinoco, I., Jr. (1988) *Proc. Natl. Acad. Sci. U.S.A. 85*, 6252−6256.
59. Lowe, L. G., and Guengerich, F. P. (1996) *Biochemistry 35*, 9840−9849.
60. Kunkel, T. A. (1990) *Biochemistry 29*, 8003−8011.
61. Garcia, A., Lambert, I. B. and Fuchs, R. P. P. (1993) *Proc. Natl. Acad. Sci. U.S.A. 90*, 5989−6003.
62. Miller, H., and Grollman, A. P. (1997) *Biochemistry 36*, 15336−15342.
63. Goodman, M. F., Cai, H., Bloom, L. B., and Eritja, R. (1994) *Ann. N.Y. Acad. Sci. 726*, 132−143.
64. Shukla, R., Jelinsky, S., Liu, T., Geacintov, N. E., and Loechler, E. L. (1997) *Biochemistry 36*, 13263−13269.
65. Shukla, R., Geacintov, N. E., and Loechler, E. L. (1999) *Carcinogenesis 20*, 261−268.
66. Burnouf, D., Koehl, P. and Fuchs, R. P. P. (1989) *Proc. Natl. Acad. Sci. U.S.A. 86*, 4147−4151.


BI010005O